Design of an IGBT-based LCL-Resonant Inverter for High-Frequency Induction Heating

Sibylle Dieckerhoff, Michael J. Ryan and Rik W. De Doncker
Institute for Power Electronics and Electrical Drives
RWTH-Aachen
Jaegerstrasse 17-19
52066 Aachen, Germany

Abstract-A power electronic inverter is developed for a high-frequency induction heating application. The application requires up to 160kW of power at a frequency of 100kHz. This power-frequency product represents a significant challenge for today's power semiconductor technology. Voltage source and current source inverters both using ZCS or ZVS are analyzed and compared. To attain the level of performance required, an LCL load-resonant topology is selected to enable ZVS close to the zero current crossing of the load. This mode of soft-switching is suitable to greatly reduce the IGBT losses. Inverter control is achieved via a Phase Locked Loop (PLL). This paper presents the circuit design, modeling and control considerations.

I. INTRODUCTION

The load in induction heating applications generally turns out to have a very low power factor. To compensate reactive power, the inductive load is extended to a resonant tank by adding further capacitive and sometimes inductive devices. Previous publications focus on simple series or parallel resonant circuits, often including a matching transformer [1-4]. In the following, an IGBT-converter supplying a third order resonant tank is presented. This solution enables the adaptation to a varying load while avoiding the transformer. A basic study of the chosen *LCL* resonant circuit has already been presented in [5,7], and a feasible control scheme is given in [6]. This paper will put the main stress on a detailed, application-specific analysis of the circuit to obtain design rules for active and passive components. A control scheme to match the demands and characteristics of the present load is derived.

The induction heating application discussed in this paper requires high active power (more than 100kW) and at the same time operates at frequencies around 100kHz. There are other induction heating applications mentioned in the literature that make similar demands on the power supply. Due to the high frequency, the suggested converters are mainly set up with MOSFETs [2-7]. This is an economically feasible solution only for lower power requirements. The developments in IGBT-technology make it possible to build more compact and cheaper converters for higher frequencies using IGBTs. The solution presented in [8] consists of a voltage source inverter that is coupled to a series resonant load via a transformer. In [9], a current source inverter drives a parallel resonant circuit. In section II, it will be shown that for the present application, the voltage source inverter with the *LCL* resonant tank has an advantage over the current

source inverter, especially when IGBTs are the chosen active devices.

II. CONVERTER TOPOLOGIES

A. Load Characteristics

The induction heating coil in the present application is used to heat various steels. The simple equivalent circuit describing the system consists of a coil and a resistor connected in series. The power factor of the system may change with the load between approximately 0.03 and 0.08. Hence, the required reactive power is extremely high: between 2MVA and 5MVA for 160kW active power. In the equivalent circuit, this change is due to the change in the resistor value, whereas the inductance of the coil does not vary significantly with the load.

Safety requirements restrict the inductor voltage to an upper limit of 3kV, and hence the rated inductor current is above 1kA. It is necessary to have reactive power compensation with a capacitor bank connected in parallel to the coil, because it is not desirable to stress the active devices in the inverter with currents as high as 1kA. The compensation reduces the current in the inverter to approximately 250A.

B. Feasible Converter Topologies

With the switching times of today's high-voltage IGBTs being still quite high, 1200V IGBTs were chosen for the 100kHz application. These IGBTs can operate at a 800V dc-link voltage. Therefore, a voltage boost is necessary to obtain the required voltage of maximal 3kV at the inductor. In addition, the voltage and current in the resonant circuit vary with different loads. Hence, voltage adaptation is often required when working with the full dc-link-voltage at rated power. To avoid a transformer, these demands result in the design of a third order resonant circuit with switchable passive devices. Figure 1 shows the two feasible solutions for the inverter and the resonant circuit: a current-source inverter with capacitive coupling and a voltage source inverter with inductive coupling of the load. Neglecting parasitics and assuming ideal semiconductor switches, both inverters would at best operate with output voltage and current in phase.

The principle of duality for the series and the parallel resonant converter can be extended to the modifications of these basic circuits, topologies A and B. This includes the desired characteristics of the switching devices, the necessary dc link, the switching control and also the behavior of the
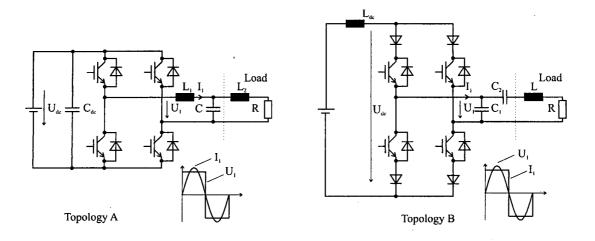
Topology A

Topology B

Fig. 1. VSI with inductive coupling (topology A) and CSI with capacitive coupling (topology B) of the load

circuits in case of a failure. Table I summarizes the features of both topologies. Especially interesting is the steady state operating point. It is derived by a fundamental component analysis of the ideal, lossless resonant LCL- respectively CCL-tank.

The value of the complex input impedance $\underline{Z}$ of the resonant tank defines the two resonant angular frequencies ω_{01} and ω_{02}. They can be found by calculating those frequencies which result in either infinite or zero input impedance. The following equations show the results of this analysis:

$$\text{Topology A } (LCL) \qquad \text{Topology B } (CCL)$$

$$\underline{Z} \rightarrow 0 \quad \omega_{01} = \frac{1}{\sqrt{C \cdot L_1 L_2 / (L_1 + L_2)}} \quad \omega_{01} = \frac{1}{\sqrt{L \cdot C_2}}$$

$$\underline{Z} \rightarrow \infty \quad \omega_{02} = \frac{1}{\sqrt{C \cdot L_2}} \quad \omega_{02} = \frac{1}{\sqrt{L \cdot C_1 C_2 / (C_1 + C_2)}}$$

$$(1)$$

The LCL resonant tank is supplied by a voltage source inverter. It operates at the resonant frequency defined by the complex input impedance $\underline{Z} \rightarrow 0$, which is the resonance point of a series resonant circuit. For the CCL-tank, the opposite statement is valid: the resonant circuit works at the frequency set by the input impedance $\underline{Z} \rightarrow \infty$ and therefore at the resonance point of an equivalent parallel resonant circuit.

C. Comparison of Converter Topologies

Different aspects have to be considered to perform a comparison of the two solutions. Of special interest are
- the mode of soft switching and the losses in the active devices;
- the effect of parasitic inductance and capacitance on circuit design and control and on the stress of devices;
- the design of the dc link;
- the design of resonant passive devices;
- the fault handling;
- the flexibility of the solution.

Table II gives an overview of the most important advantages and disadvantages of the voltage source and the current source topology. In the evaluation special focus has been made on the overall system and especially the semiconductor losses. Theoretically, soft switching of the IGBTs can easily be achieved with aid of the resonant load. However, the switching losses are still dominant at 100kHz switching frequency and limit the overall performance of the system. Hence, the first aim is to find the solution with the lowest switching losses. Both topologies allow ZCS or ZVS. The mode of operation is set in advance by circuit parasitics and nonideal device characteristics.

In the voltage source inverter, the output capacitance C_{CE} of the IGBTs influences the switching instant: switching at the zero-crossing of the current leads to additional turn on

Table I
DUALITY OF TOPOLOGIES A AND B

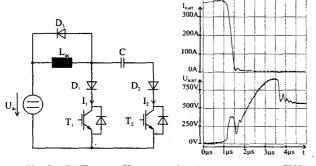| Topology A (LCL resonant tank)	Topology B (CCL resonant tank)
Voltage source inverter	Current source inverter
Bidirectional current flow through semiconductors	Bidirectional voltage blocking capability of semiconductors
Rectangular output voltage, sinusoidal output current	Rectangular output current, sinusoidal output voltage
Dead time required for the commutation process	Overlap time required for commutation process
Switching instant slightly before zero crossing of the load current	Switching instant slightly before zero crossing of the load voltage
Inverter has to be switched off in case of a short circuit	All semiconductors must conduct in case of a short circuit, a crowbar or energy recovery is required
Operation frequency approximately $\omega = \frac{1}{\sqrt{C \cdot L_1 \cdot L_2 / L_1 + L_2}}$	Operation frequency approximately $\omega = \frac{1}{\sqrt{L \cdot C_1 \cdot C_2 / C_1 + C_2}}$

2040

TABLE II
COMPARISON OF FEASIBLE CONVERTER TOPOLOGIES

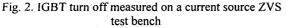| VSI with inductive coupling of the load (LCL resonant tank)		CSI with capacitive coupling of the load (CCL resonant tank)	
+	Zero-current soft-switching at resonant frequency.	+	Zero-voltage soft-switching at resonant frequency.
+	Zero-voltage soft-switching above resonant frequency.	+	Zero-current soft-switching above resonant frequency.
+	Good usage of voltage-blocking capability of the IGBTs resulting in low conduction losses.	–	Due to the sinusoidal voltage waveforms the blocking capability of the IGBTs is poorly used resulting in higher currents and consequently leading to higher losses.
+	IGBTs are standardized for usage in voltage source inverters.		
+	No additional series diodes necessary.	–	Additional series diodes necessary as high-speed symmetric devices are not yet available.
		±	The stray inductance in the supply conductor from the inverter to the load is critical (overvoltages across the IGBTs, higher switching losses); compensation is possible (with limitations) by an optimized switching strategy, similar to the natural commutation in thyristor bridges [10].
+	The resonant capacitor can be placed close to the inductor thus reducing losses by minimizing the length of the high-voltage, high-current connection.	–	To minimize the stray inductance in the cable between inverter and load, the capacitor bank is split with the parallel capacitor close to the inverter. This leads to high losses and voltage drops across the connection.
–	Design of the output resonant coil is difficult, taking care of leakage fields and losses.		
–	DC link design must be of extremely low inductance.	+	Design of the DC link is not critical.
		+	Better short-circuit and no-load handling capability because of the current-limiting DC link.

losses because of the discharging of the capacitance C_{CE} . Switching below the resonant frequency, i.e., after the zero-crossing of the current means current-commutation from the opposite diode. This mode of operation should be avoided in each case, because of possible current and voltage peaks due to the reverse recovery effect of the diode. The high-frequency inverter is equipped with very fast drivers to reduce switching times and therefore the aforementioned effect is very strong. Hence, a lagging current, i.e. a slightly inductive load characteristic, is the desired mode of operation, because ZVS can be realized.

The output stray inductance is the critical parameter in the current source inverter. It is especially important when high flexibility of the converter system is required. This means that there may be quite a long (several meters) distance between the inverter and the resonant load with significant stray inductance. To illustrate the problem, fig. 2 shows a measurement of IGBT voltage and current during turn off. The device under test is the IGBT T_1 .The measurement was carried out on a current source test bench allowing zero-

voltage switching. This test bench was proposed for the evaluation of GTOs and it is explained in detail in [11,12]. Here, a 1200V, 500A IGBT with punch-through technology was tested. The picture clearly depicts the problem of switching losses owing to the stray inductance in the current source inverter. To avoid the voltage peak, it is recommended to switch the next IGBT before the zero crossing of the sinusoidal voltage. This operation mode is similar to the well known natural commutation process in thyristor bridges. The optimal phase angle between voltage and current is derived when we assume that the commutation of the current is finished at the zero-crossing of the voltage. The formula (2) to determine the optimal switching angle β is given in [10]. It depends on the stray inductance L_{stray} , the inverter current I_1, the inverter voltage U_1 and the angular frequency ω :

$$\cos \beta = 1 - \frac{2 \cdot L_{stray} \cdot I_1 \cdot \omega}{U_1}. \qquad (2)$$

This kind of control has two disadvantages: first, it varies with the load, the circuit setup and the frequency and therefore it is difficult to adjust exactly to the desired switching instants. Secondly, the larger the overlap angle $\phi = 180° - \beta$ of the commutation, the higher the kVA-rating of the inverter to achieve constant real power at the load, thus leading to higher semiconductor losses. Hence, this control scheme only makes sense for low parasitic inductive setups but does not match the feature of a flexible system for induction heating.

Further results of the comparison of the two topologies are summarized in table II. Based on this comparison, topology A was found to be the most suitable solution for the application at hand with using present IGBT devices. Details on the circuit and the control scheme are presented in the following sections.
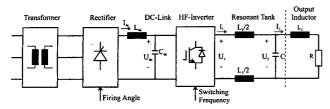

Fig. 2. IGBT turn off measured on a current source ZVS test bench

Fig. 3. High-frequency induction heating system with LCL-resonant output

III. SYSTEM ANALYSIS

The entire induction heating system is shown in the block diagram of Fig. 3. On the input side, the high-frequency IGBT-inverter is connected to a thyristor rectifier via a voltage link. The inverter supplies a resonant $LCLR$-load with an LC-circuit coupling the output inductor to the inverter. This LC-circuit serves two purposes:

1. It provides the reactive current drawn by the output inductor and
2. it provides a significant voltage boost across the L_1 inductor.

A. Impedance Characteristics

A fundamental component analysis of the resonant load gives good insight into the circuits characteristics. A very useful variable to determine the characteristics is the complex input impedance $\underline{Z}$ of the $LCLR$-circuit. In terms of impedance, the purpose of the inductor L_1 is to transform the rather low impedance of the compensated output inductor ($Z \approx R \approx 0.1\Omega$) to a more suitable value for the inverter ($Z \approx R_{eq} \approx 3.2\Omega$) while working close to the resonant frequency set by L_1, L_2 and C. The complex impedance $\underline{Z}$ consists of the real part

$$R_{eq} = \frac{R}{\left(1 - \omega^2 L_2 C\right)^2 + \left(\omega RC\right)^2} \qquad (3)$$

and of the imaginary component

$$X_{eq} = \omega L_1 + \frac{\omega L_2 - \omega^3 L_2^2 C - \omega R^2 C}{\left(1 - \omega^2 L_2 C\right)^2 + \left(\omega RC\right)^2}. \qquad (4)$$

As the IGBTs are switched close to the zero crossing of the load current, the analysis can be simplified further, when we assume that the fundamental components of the inverter output voltage and current are approximately in phase. Therefore, $X_{eq} \approx 0$, and the inverter is designed to supply the required real power P_{Load} to the load:

$$P_{Load} = P_{Inverter} = \frac{\tilde{U}_1^2}{R_{eq}}. \qquad (5)$$

In (5), the voltage $\tilde{U}_1$ is the rms-value of the inverter rectangular output voltage. With the output power of the inverter $P_{Inverter}$ being equal to the load power P_{Load} , the transformation ratio between the absolute values of the inverter current I_1 and the inductor current I_2 is simply set by

the ratio of the resonant tank equivalent input resistance and load resistance:

$$\frac{I_2}{I_1} = \sqrt{\frac{R_{eq}}{R}} . \qquad (6)$$

For a resonant tank with a high quality factor Q, the approximation

$$\frac{I_2}{I_1} = \frac{L_1}{L_2} \qquad (7)$$

given in [7], is valid for the resonance point defined by $\underline{Z} \rightarrow 0$. This relationship gives an idea of the necessary size of the inductor L_1 . A rough design of the resonant tank is achieved when the value of the capacitor C is set by applying (1).

The load power and the phase demand, together with the desired resonant frequency range, fix the values of the resonant passive components L_1 and C. For a more exact design of the circuit it makes sense to proceed as follows:

1. Calculate the equivalent input resistance R_{eq} of the resonant tank for nominal power and nominal dc-link voltage.
2. Set the resonant angular frequency ω.
3. With 1. and 2. calculate the capacitance C.
4. Adjust L_1 for $X_{eq} \approx 0$ or exactly for the desired phase lag ϕ between inverter voltage and current. (See [5] for a detailed explanation.)

B. Parameter Variation

The basic inverter design is done for rated power and a given load. In the real application, the system must be capable of controlling load power, and it must cope with load variations that may occur during startup and when various steels are heated within the same inductor. Concerning the power control, it is either possible to modify the switching frequency or to vary the dc-link voltage. The optimum phase lag ϕ with regard to minimal switching losses fixes the switching frequency for a given resonant tank. Hence, frequency variation is not a feasible control solution, and the output power has to be controlled by the rectifier adjusting the dc-link voltage.

The load variation during startup is expressed by the change in the equivalent resistance R_{eq} which, based on (6) and (7), is approximately
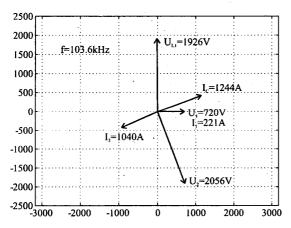
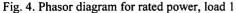$$R_{eq} \cong R \cdot \left(\frac{L_1}{L_2}\right)^2 . \qquad (8)$$

The equivalent resistance of the cold load is smaller than the nominal value. Therefore, the rectifier control reduces the power of the circuit during startup so that the rated inverter current is not exceeded.

As already mentioned in section II, the load power factor changes with the type of the steel that is processed. The variation of the power factor is due to the variation of the load resistance, whereas the inductance L_2 remains practically

constant. To attain rated power for each load, the resistance R_{eq} must always possess its nominal value. Assuming the parallel capacitor C is unchangeable, the resonance angular frequency ω is changed and the inductance L_1 is modified to set the desired phase angle ϕ. This solution is permissible because the frequency does not vary significantly in this application. Table III contains equivalent system data at rated power for the heating of two different steels. The inductor data L_1 and R are based on simulations. Figures 4 and 5 depict the corresponding phasor plots assuming $\phi = 0$.

Table III
SYSTEM DATA

	Load 1	Load 2
Power Factor	0.077	0.035
Rated Power P_N	160kW	160kW
Eq. Resistance R_{eq}	3.24Ω	3.24Ω
Inductance L_2	3.03μH	2.90μH
Resistance R	147mΩ	63mΩ
Capacitance C	0.93μF	0.93μF
Inductor L_1	13.4μH	20.2μH
Resonant frequency f_{02}	103.6kHz	103.2kHz
L_1 based on (8)	14.2μH	20.8μH
f_{02} based on (1)	104kHz	103kHz

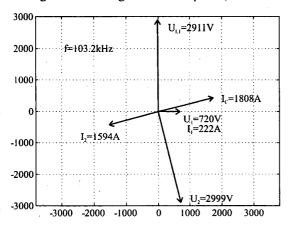Fig. 4. Phasor diagram for rated power, load 1

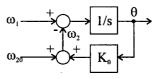Fig. 5. Phasor diagram for rated power, load 2

IV. INVERTER CONTROL

The control of the switching instants with a frequency of 100kHz is too high to be implemented with a DSP or a micro-controller. Hence, a control scheme based on an analog Phase Locked Loop (PLL) has been chosen. In combination with an integrator, the PLL adjusts to the desired phase angle between the output voltage and current of the inverter, and supplies the IGBT-driver stages with the switching signals.

A. Basic Design Considerations

Figure 6 shows the phase angle ϕ between I_1 and U_1 as a function of frequency. This phase angle is not monotonic but changes from inductive to capacitive to inductive. Therefore, it is not suitable for a control variable. Instead, [6] proposes to use the phase angle θ between the output voltage U_1 and the voltage U_2 across the parallel resonant circuit. θ has also been drawn in Fig. 6. In the interesting frequency range above the second resonant frequency f_{02}, the slopes of the phase angles θ and ϕ are approximately the same.

B. Load Model

Fundamentally, the angle θ is the integration of the frequency difference ($\omega_1 - \omega_2$) between the switching angular frequency ω_1 and the angular frequency of U_2, ω_2. Note that unlike in section A, in the following sections θ and ϕ represent phase lags with positive values. To model the steady state relation between θ and ω_1, as depicted below, a negative feedback term K_θ is added around the integrator, with an offset value of ω_{02}. The model represents a linearization of the $\theta = f(\omega)$ relationship around an operation point, where K_θ represents the slope, and ω_{02} the intercept.

The small signal characteristics of the model may be described by the transfer function in Laplace form,
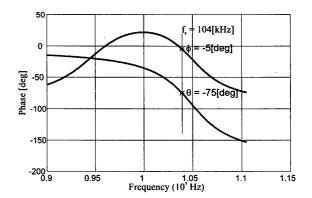

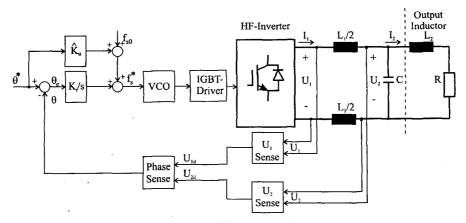Fig. 6. Relation between the phase $\phi (I_1/U_1)$ and the phase θ (U_2/U_1) of the $LCLR$-tank

Fig. 7. Basic Phased Locked Loop Structure

$$\frac{\theta}{\omega_1} = \frac{1}{K_\theta + s} = \frac{\tau_\theta}{\tau_\theta \cdot s + 1}, \qquad (9)$$

where the time constant $\tau_\theta = 1/K_\theta$. Note that for the LCL parameters given in table III, the load has natural "open-loop" response of around 3kHz.

C. Control Structure

Figure 7 explains the basic Phase Locked Loop structure. In evaluating the transient response desired for the controller, it was determined that the inherent open-loop response of the load would be more than adequate to track any anticipated disturbances. Thus, aside from decoupling and feed-forward terms, only an integral gain controller was needed. This had the added benefit of eliminating the need for a low-pass filter on the phase-angle feedback signal, as is needed in most PLL controllers.

To obtain the control variable θ, the voltages U_1 and U_2 are measured, converted into digital signals U_{1d}, U_{2d} and processed by an XOR element. The average output voltage of the phase sensor $\overline{U}_\theta$ is proportional to the absolute value of the phase shift. The difference between the measured value and the setpoint value U_θ^* is integrated. In addition, a feed forward control allows presetting the operating frequency. The deviation due to the phase error is added to the working
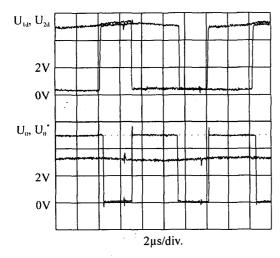
frequency and fed into a VCO. The VCO's rectangular output signal drives the IGBT driver stages. The measurements in fig. 8 illustrate the principle of the PLL. The upper curves show the digital input signals of the phase sense, the lower curves depict the output voltage U_θ of the XOR element and the setpoint voltage. In steady state, the average voltage $\overline{U}_\theta$ equals the setpoint value.

D. Experimental Verification of Control Design

The control design has been verified with the help of a low power IGBT-inverter operating at approximately 70kHz. The
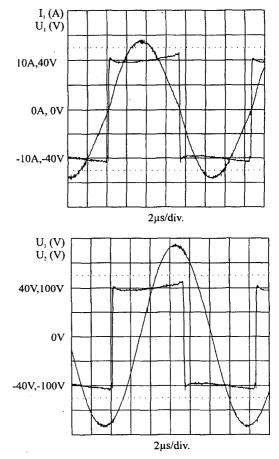

Fig. 9 . Current I_1 and voltages U_1, U_2 for $\phi \approx 0°$, $\theta \approx 68°$

Fig. 8.Principle operation of PLL ($\phi \approx 0°$, $\theta \approx 68°$)

electrical characteristic of the laboratory model was scaled to match the phasor characteristics of the real system shown in fig.4. Figure 9 depicts the current (I_1) and voltage waveforms (U_1, U_2) for operation at resonance. In the upper diagram we find voltage and current in phase, the lower diagram presents the phase shift θ.

V. SUMMARY

In this paper, the design of an IGBT-based power supply for an induction heating system has been presented. The variable load is highly inductive and requires a 160kW active power at a frequency of 100kHz. Based on a detailed topology investigation, a third-order LCL-resonant circuit supplied by a voltage source H-bridge-inverter is chosen. An analysis of the circuit and basic design rules are given. A control scheme allowing operation of the inverter with the lowest IGBT switching-losses is explained and experimental results verifying the operation of the control are shown.

REFERENCES

[1] K. Mauch: "Transistor Inverters for Medium Power Induction Heating Applications", IEEE IAS 1986, pp. 555-562

[2] S. Bottari, L. Malesani, P. Tenti: "High Efficiency 200kHz Inverter for Induction Heating Applications", IEEE PESC 1985, pp. 308-316

[3] E. J. Dede, J. V. Gonzalez, V. Esteve, J. A. Linares, J. Jordan, D. Ramirez, E. Maset: "25kW/200kHz Parallel Resonant Converter for Induction Heating", ETEP-Journal Vol.2, No.2 1992, pp. 103-109

[4] P. Casella, Pham Huu Phut, A. Berthon: "High Frequency Current Inverter with Parallel Resonant Load for Induction Heating", EPE 1987, pp. 277-280.

[5] G. L. Fischer, H. Dort, H. Knaak, G. Amler, B. Hemmer: "Resonance Transformation for Induction Heating", PCIM Europe, March/April 1994, pp. 76.-79

[6] H. Dort, G. Birk, G. L. Fischer: "Control Mode for Inverters with Resonance Transformation in Induction Heating Applications", Proc. Power Conversion, June 1994, pp. 57-67

[7] G. L. Fischer, H. Dort: "An Inverter System for Inductive Tube Welding utilizing Resonance Transformation", IEEE IAS 1994, pp. 833-840

[8] H. G. Matthes, R. Jürgens: "1.6MW 150kHz Series Resonant Circuit Converter incorporating IGBT Devices for Welding Applications", International Induction Heating Seminar 1998, pp. 25-31

[9] E. J. Dede, V. Esteve, J. Jordan J. V. Gonzalez, D. Ramirez: "Design Considerations for Induction Heating Current Fed Inverters with IGBTs Working at 100 kHz", IEEE APEC Conference Record 1993, pp. 679-685

[10] E. J. Dede, V. Esteve, J. Jordan, J. V. Gonzalez, E. Maset: "On the Design of High Power Current-Fed Inverters for Tube Welding Applications", Proc. Power Conversion, June 1993, pp.62-69

[11] A. Mertens, H.-Ch. Skudelny: "Operation and Control Requirements for a GTO used in a Parallel Resonant Inverter for Induction Heating", EPE 1989, pp. 268-273

[12] A. Mertens, H.-Ch. Skudelny: "Switching Losses in a GTO Inverter for Induction Heating", IEEE PESC 1989, pp. 298-305

[13] A. Okuno, H. Kawano, J. Sun, M. Kurokawa, A. Kojina, M. Nakaoka: "Feasible Development of Soft-Switched SIT Inverter with Load-Adaptive Frequency-Tracking Control Scheme for Induction Heating", IEEE Transactions on Industry Applications 1998, pp. 713-718